Research Article

Ghada ALMisned, Duygu Sen Baykal, Gokhan Kilic, Gulfem Susoy, Hesham M. H. Zakaly, Antoaneta Ene*, and Huseyin Ozan Tekin*

Assessment of the usability conditions of Sb_2O_3–PbO–B_2O_3 glasses for shielding purposes in some medical radioisotope and a wide gamma-ray energy spectrum

https://doi.org/10.1515/arh-2022-0133
received October 21, 2022; accepted November 21, 2022

Abstract: We report some fundamental gamma-ray shielding properties and individual transmission factors (TFs) of five distinct glass samples with a nominal composition of $x$$Sb_2O_3$·(40 − x)PbO·60B_2O_3·0.5CuO and (where; 0 ≤ x ≤ 40 mol%). Phy-X/PSD and MCNPX (version 2.7.0) Monte Carlo code are utilized to determine several critical parameters, such as cross-sections, attenuation coefficients, half and tenth value layers, build-up factors, and TFs. A general transmission setup is designed using basic requirements. Accordingly, TFs are evaluated for several medical radioisotopes. Next, the gamma-ray shielding parameters and TFs are assessed together in terms of providing the validity of the findings. Our results showed that there is a positive contribution of increasing Sb_2O_3 amount in the glass matrix owing its direct effect to the density increment as well. This positive effect on gamma-ray shielding properties is also observed for decreasing mean free path values from S1 to S5 samples. The exposure build-up factor (EBF) and energy absorption build-up factor (EABF) values, increasing the quantity of Sb_2O_3 supplementation, resulted in a general reduction in EBF and EABF values (i.e., from 0.5 to 40 mfp). When the quantity of Sb_2O_3 rises from S1 to S5, the collision rate of incoming gamma rays in glass samples increases significantly. The TF figures reveal that S5 showed the least transmission behavior across all the above-mentioned studied glass thicknesses. It can be concluded that increasing the Sb_2O_3 additive is a beneficial and monotonic technique, when the gamma-ray shielding qualities or TF values must be further enhanced.

Keywords: Sb_2O_3/PbO/B_2O_3 glasses, Phy-X/PSD, MCNPX, radiation shielding

* **Corresponding author: Antoaneta Ene,** Department of Chemistry, Physics and Environment, INPOLDE Research Center, Faculty of Sciences and Environment, Dunarea de Jos University of Galati, 47 Domneasca Street, 800008 Galati, Romania, e-mail: Antoaneta.Ene@ugal.ro
* **Corresponding author: Huseyin Ozan Tekin,** Department of Medical Diagnostic Imaging, College of Health Sciences, University of Sharjah, 27272, Sharjah, United Arab Emirates; Computer Engineering Department, Istinye University, Faculty of Engineering and Natural Sciences, Istanbul 34396, Turkey, e-mail: tekin765@gmail.com
Ghada ALMisned: Department of Physics, College of Science, Princess Nourah Bint Abdulrahman University, P.O. Box 84428, Riyadh 11671, Saudi Arabia
Duygu Sen Baykal: Department of Medical Imaging Techniques, Vocational School of Health Sciences, Istanbul Kent University, Istanbul, 34433, Turkey
Gokhan Kilic: Department of Physics, Eskisehir Osmangazi University, Faculty of Science and Letters, Eskisehir, TR-26040, Turkey
Gulfem Susoy: Department of Physics, Faculty of Science, Istanbul University, Istanbul 34134, Turkey
Hesham M. H. Zakaly: Institute of Physics and Technology, Ural Federal University, 620002 Ekaterinburg, Russia; Physics Department, Faculty of Science, Al-Azhar University, Assiut 71524, Egypt

1 Introduction

Radiation shielding is not a matter of choice but rather a strictly regulated legal procedure. Selecting the most appropriate shielding barriers is also a very significant necessity, even though the functioning of this process is achievable with the enlightened knowledge of the employees and the society [1,2]. This is because ionizing radiation is being used more often in scientific and technological endeavors as well as in the treatment of disease in humans. The benefits of this radiation type are being employed in energy production, radiotherapy, medical diagnostics, nuclear power, and other industrial processes. Time, distance, and shielding are the three primary concepts in radiation protection. Increasing a shielding material's

capacity to soak up various forms of ionizing radiation [3] might improve its effectiveness. The most effective shielding materials have often been made of lead (Pb). Novel targeted radioisotopes have led to the widespread use of radioisotope therapy in nuclear medicine clinics, especially for the treatment of cancer. It is important for nuclear medicine facilities to have certain timing, distance, and shielding characteristics in place to reduce radiation exposure to both staff and patients [3,4]. These goals include increasing exposure to radioactive sources among workers, patients, and the public; keeping all radioisotope and radiopharmaceutical activity under tight supervision; and preventing the spread of contamination [5–7]. Because of these drawbacks, researchers have been working hard to manufacture next-generation shielding materials that could be an improvement over the current crop [8]. Glass is a valuable radiation barrier due to its ability to absorb gamma rays and neutrons, as well as its transparency and simplicity of compositional modification. Borate glasses are essential optical materials owing to their low melting temperatures, excellent transmittance, and good thermal stability [9]. Typically, they are used in the production of insulating and dielectric materials. Adding transition metal ions to their structure, however, results in semi-conductivity. Due to their existence in two or more valence states, which influences structural and optical properties [10–17], transition metals are widely employed in glasses at present. In addition to optical and structural properties of borate glasses, studies reported that their radiation shielding properties are quite satisfactory as proportional to their ratios when they are doped with transition metals [18–20]. Moreover, boron has neutron capture property and in addition to doping concrete with boron [21] and glasses also benefited from this property. Studies related to the binary glass that B_2O_3 forms when merged with PbO are mostly on the investigation of structural properties [22]. However, the unique property of PbO in respect to shielding gamma and X-rays, and furthermore, boron's success in capturing neutrons revealed that the glass structure that these two elements form together might have an important place in radiation shielding. However, since the density of the final composition would be relatively lower compared to PbO, there are studies in the literature on the enrichment of glass by doping with different elements and especially improvement of the density is encountered [23,24]. Glasses containing heavy metal oxides such as Sb_2O_3 are frequently being investigated due to their unique transmittance properties in the infrared region in the field of optics [25]. Studies on the impact of glasses containing heavy metal oxides on radiation shielding are increasing with each passing day [26,27]. Studies on the impact of the presence of both PbO and Sb_2O_3 oxide compounds within the same glass structure on radiation shielding properties set forth interesting results [28,29]. In this work, we provide the results of a complete examination of the optically defined $x$$Sb_2O_3$·(40 − x)PbO·60-B_2O_3·0.5CuO (where, $0 \le x \le 40$ mol%) glass systems. This study's results provide insight into how the addition of Sb_2O_3 to the glass compositions under study led to a proportionate increase in absorption, which might be valuable in assessing the materials created in the cited article on a larger scale.

2 Materials and methods

2.1 Glass characterization

Based on the previous research, seven samples of tungsten/barium/phosphate glasses having the chemical formula $x$$Sb_2O_3$·(40 − x)PbO·60B_2O_3·0.5CuO and (where, $0 \le x \le 40$ mol%) increments were chosen for this inquiry. A previous study of this class of materials [30] examined the parameters of gamma-ray absorption for a restricted energy range. The TF factors are estimated in this study by utilization of the gamma-ray energies of nuclear-type radioisotopes. This research will provide essential information for more practical applications by maintaining a much higher level for the photon energy range that is investigated in this research. This study takes into account several build-up factors as well as other essential shielding properties, both of which were omitted from earlier studies.

The following is a list of details regarding the glasses that were examined:

- S1: 0.240740B + 0.385806O + 0.003974Cu + 0.36948Pb (ρ: 5.00 g/cm^3).
- S2: 0.200616B + 0.342811O + 0.003974Cu + 0.083118Sb + 0.369480Pb (ρ: 5.20 g/cm^3).
- S3: 0.160493B + 0.299816O + 0.003974Cu + 0.166237Sb + 0.369480Pb (ρ: 5.30 g/cm^3).
- S4: 0.120370B + 0.256821O + 0.003974Cu + 0.249355Sb + 0.369480Pb (ρ: 5.50 g/cm^3).
- S5: 0.080247B + 0.213826O + 0.003974Cu + 0.332474Sb + 0.369480Pb (ρ: 5.75 g/cm^3).

Glass codes, elemental weight fractions, and density are tabulated in Table 1.

2.2 Shielding parameters and gamma transmission factors (TFs)

The ability of radiation-shielding materials to absorb a part of the initial radiation quantity that impacts an

Table 1: Sample code, elemental weight fraction, and density of $xSb_2O_3{\cdot}(40 - x)PbO{\cdot}60B_2O_3{\cdot}0.5CuO$: ($0 \le x \le 40$ mol%)

Sample code	Elemental weight fraction (wt%)					Density ρ (g/cm^3) [30]
	B	O	Cu	Sb	Pb	
S1	0.240740	0.385806	0.003974	0	0.369480	5.00
S2	0.200616	0.342811	0.003974	0.083118	0.369480	5.20
S3	0.160493	0.299816	0.003974	0.166237	0.369480	5.30
S4	0.120370	0.256821	0.003974	0.249355	0.369480	5.50
S5	0.080247	0.213826	0.003974	0.332474	0.369480	5.75

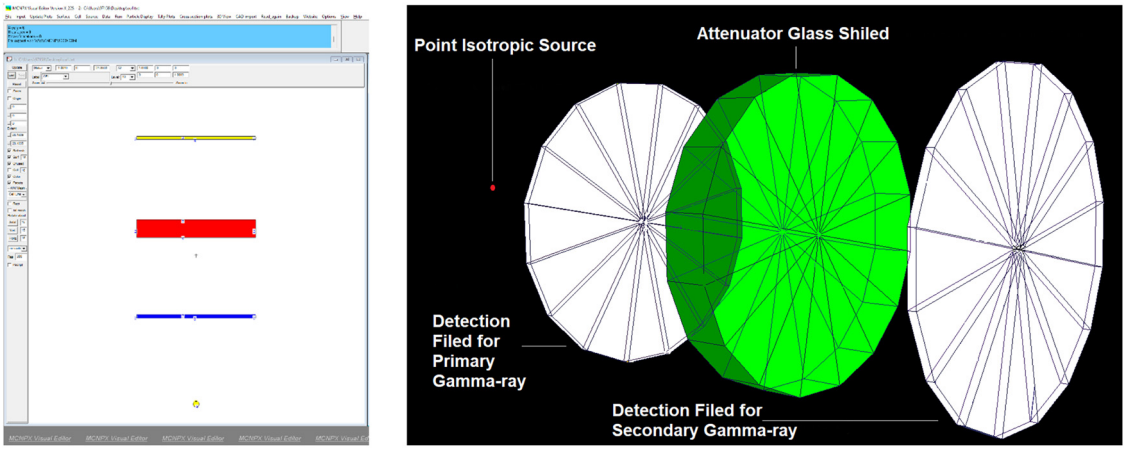

Figure 1: (a) 2-D view of designed MCNPX simulation setup. (b) 3-D illustration of designed MCNPX setup (2-D and 3-D views are obtained from MCNPX Visual Editor VisedX22S).

attenuator is a further essential characteristic. This criterion may be expressed in terms of a value determined by primary and secondary radiation quantities. The term TF [1,31,32] is a crucial parameter that enables researchers to measure the attenuation of incident gamma rays as a function of secondary gamma-ray intensity. This research analyzed the TF values of glass samples tested for a variety of radioisotopes used for nuclear-type disease therapy and

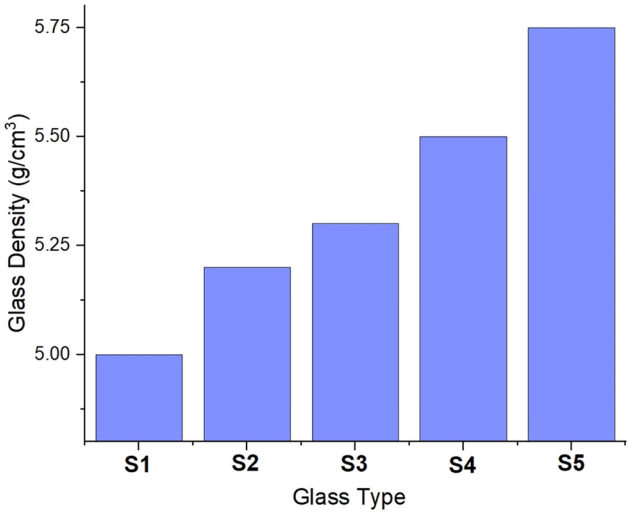

Figure 2: Variation of glass densities.

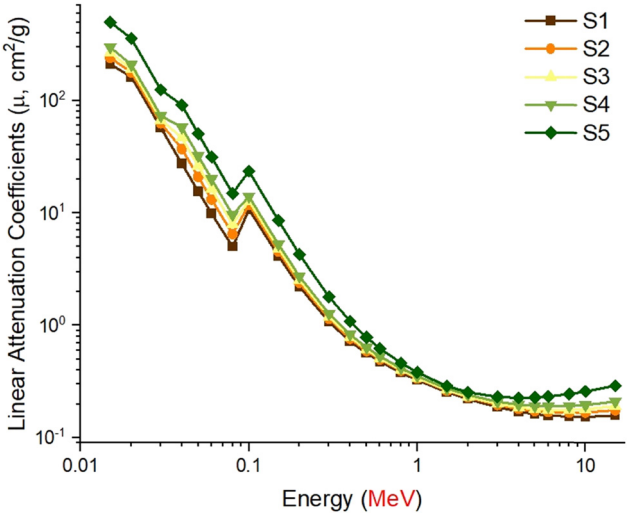

Figure 3: Variations of linear attenuation coefficient (1/cm) with photon energy (MeV) for all S1–S5 glasses.

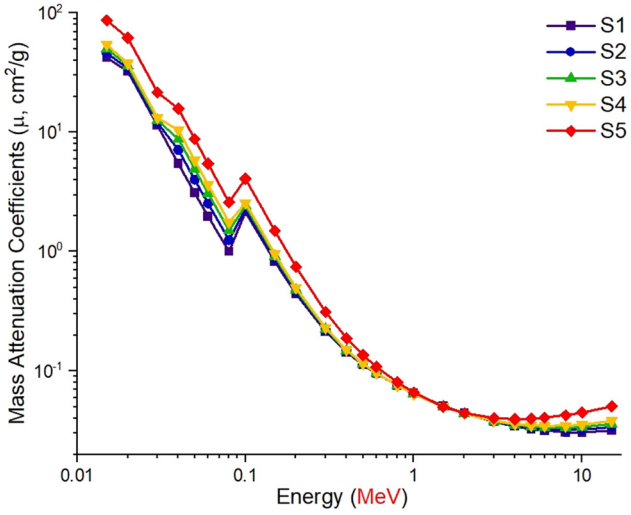

Figure 4: Variations of mass attenuation coefficients (cm^2/g) with photon energy (MeV) for all S1–S5 glasses.

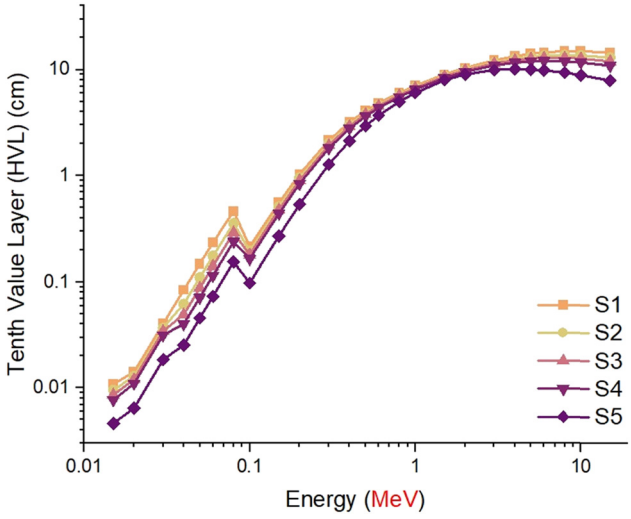

Figure 6: Variations of TVL (cm) with photon energy (MeV) for all S1–S5 glasses.

diagnostics. The radioisotopes indicated ^{67}Ga (0.0086, 0.0093, 0.1840 MeV), ^{57}Co (0.0144, 0.1221, 0.1365 MeV), ^{111}In (0.0230, 0.1710, 0.2450 MeV), ^{133}Ba (0.0532, 0.0796, 0.0810, 0.2764, 0.3029, 0.3560, 0.3838 MeV), ^{201}Tl (0.0710, 0.1350, 0.1670 MeV), ^{99m}Tc (0.1405 MeV), ^{51}Cr (0.3201), ^{131}I (0.2843, 0.3645, 0.6370, 0.7229 MeV), ^{58}Co (0.5110, 0.8108 MeV), ^{137}Cs (0.6617 MeV), and ^{60}Co (1.1732, 1.3325 MeV) specific energies [8]. This portion of the investigation simulates a large transmission assembly using the MCNPX method [33]. The MCNPX method's resulting configuration is seen in three dimensions in Figure 1. The graphic illustrates that the quantity of gamma rays that are absorbed by the glass material between the two detection zones is the most important aspect that is considered when calculating the TF values. The modeling approach was predicated on the production of the MCNPX input file, and it was considered complete when the tally values were exported from the output file and the TF values were specified.

3 Results and discussion

By computing the radiation absorption characteristics of glass materials in accordance with specified parameters, the direct contribution of structural changes to their

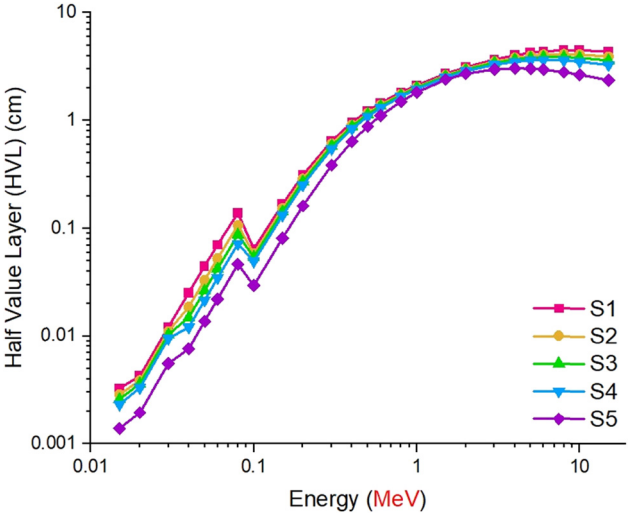

Figure 5: Variations of HVL (cm) with photon energy (MeV) for all S1–S5 glasses.

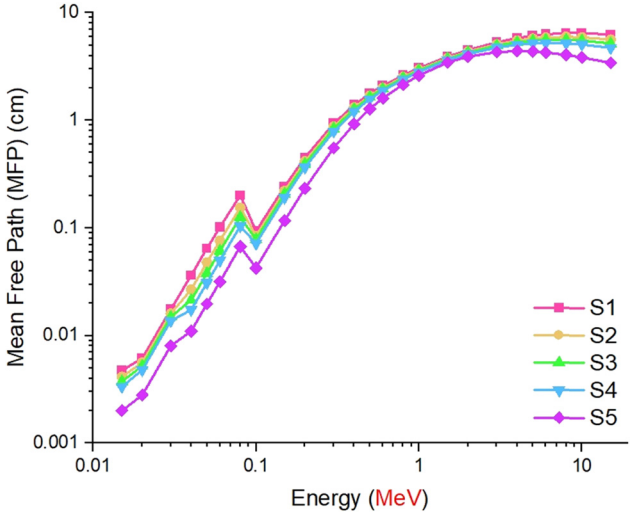

Figure 7: Variations of mean free path (cm) with photon energy (MeV) for all S1–S5 glasses.

absorption qualities may be analyzed [34–41]. The radiation attenuation properties of five different glass samples doped with varied amounts of Sb_2O_3 were investigated. The Sb_2O_3 additive ratio was raised to its highest level in the S5 sample after being raised gradually in numerous glass compositions from S1 to S5. The density of the glass samples that were examined varies as shown in Figure 2 depending on the proportion of Sb_2O_3 that is present in the overall glass composition. There was a 0.75 g/cm^3 difference in glass density between the lowest and highest Sb_2O_3 reinforcements due to the increased weight caused by the increased composition of the components. A feature of materials that shields against gamma rays is the linear attenuation coefficient (μ), which increases with increasing material density [42,43]. For any gamma-ray energy, the linear attenuation coefficient of a material may be determined, making it a crucial metric for determining many others. Figure 3 displays the variation in linear attenuation coefficients as a function of gamma rays, as measured for five different glass samples. The highest linear attenuation coefficient values may be seen in the low-energy part of the presented diagram. The fact

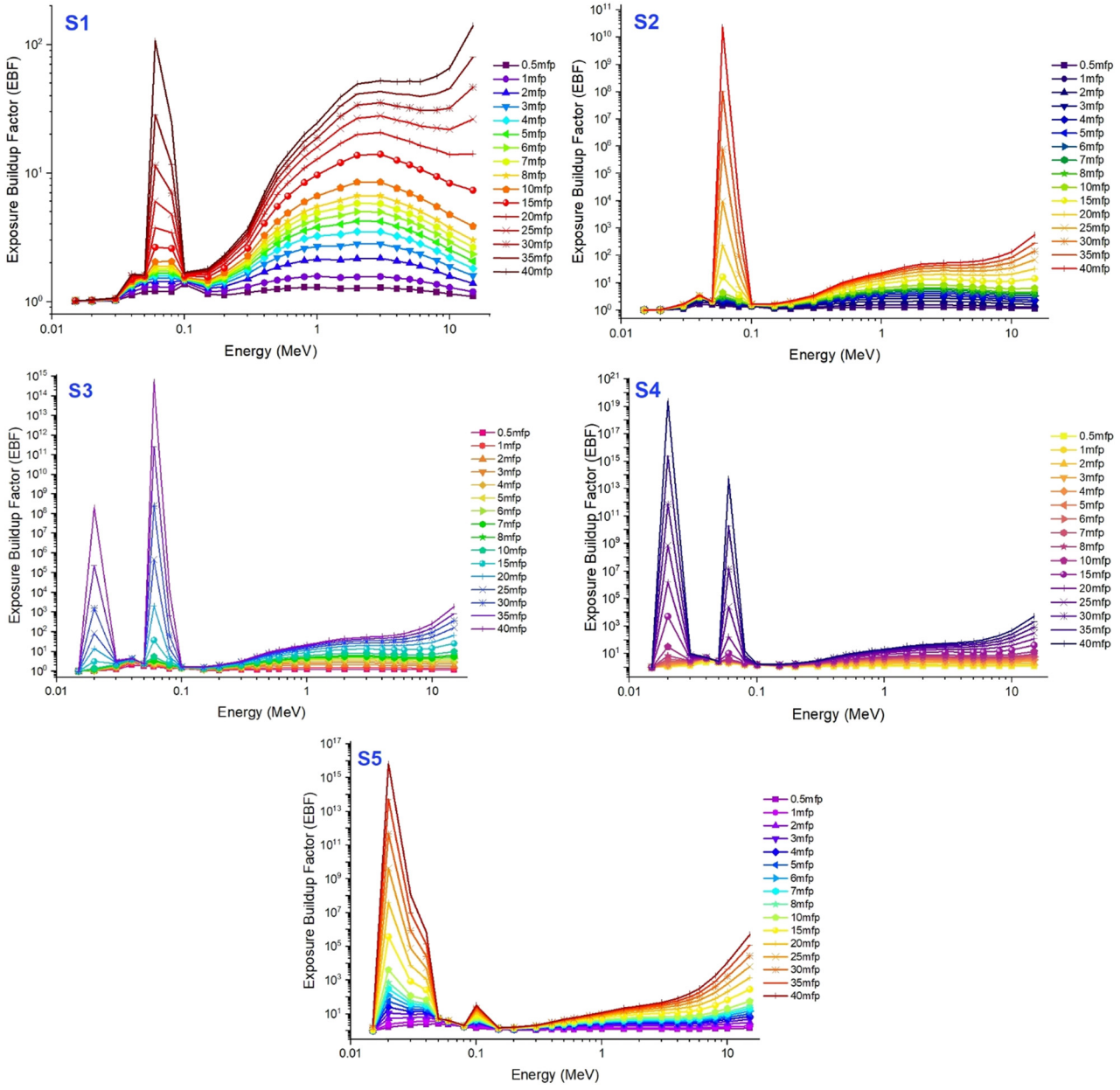

Figure 8: Variation of EBF of investigated glasses at different mean free path values.

that the k-absorption edge reached its peak and then gradually started to fade following this significant decrease in the low-energy region is evidence that Compton scattering was the predominate interaction in the mid-energy region and that the fall was followed by a lower increase. The values of the linear attenuation coefficients have been strongly impacted by the elemental compositions of the five different glass samples that were evaluated. The linear attenuation coefficients for all investigated energies were found to be highest in S5 samples with the highest Sb_2O_3 addition rate. This demonstrates that the linear attenuation coefficient of multi-glass samples improves when density rises due to Sb_2O_3 addition rate. Figure 4 depicts the variation pattern of the mass attenuation coefficient (μ_m). Overall, it was found that the linear and mass attenuation coefficients have a similar pattern. Since μ_m is a density-independent characteristic, it can be said that as the quantity of Sb_2O_3 steadily rose from S1 to S5, a clear pattern of rising m values was also seen. The linear attenuation coefficient may be used to calculate the half-value layer (HVL), a critically important feature of gamma-ray shielding [44,45]. Figure 5 shows that the HVL is a

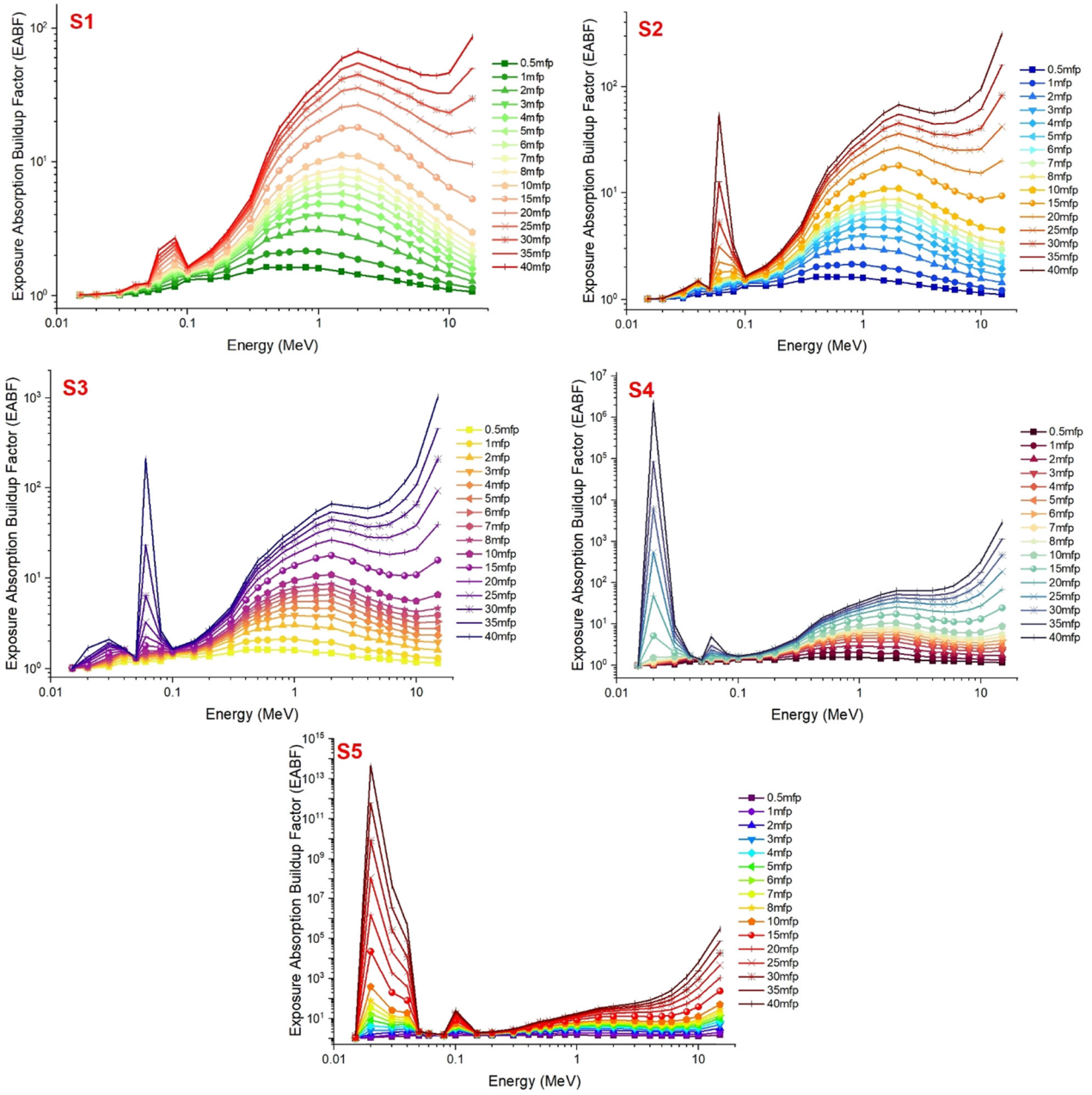

Figure 9: Variation of EABF of investigated glasses at different mean free path values.

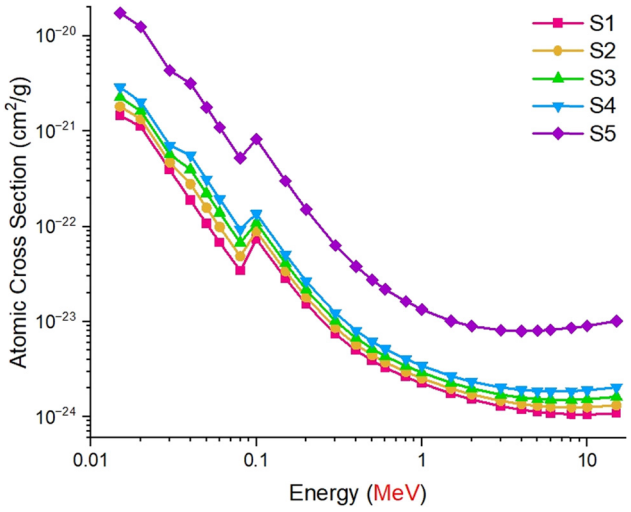

Figure 10: Variations of atomic cross-section with photon energy (MeV) for all S1–S5 glasses.

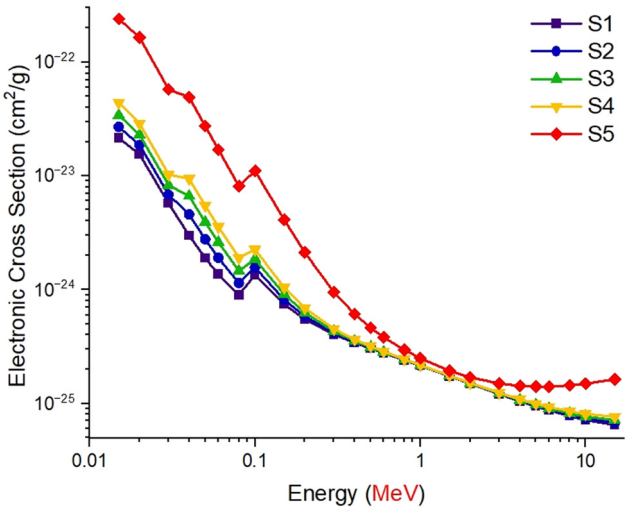

Figure 11: Variations of electronic cross-section with photon energy (MeV) for all S1–S5 glasses.

tangible depiction of the thickness at which the energy of a photon impinging on a material is decreased by half. This indicates that the gamma-ray attenuation capabilities of materials with a small half-value thickness are preferable. In other words, a material's ability to shield against a certain photon energy is improved by decreasing its HVL value. HVL values between 0.015 and 15 MeV are shown in Figure 5 for each of the seven glass samples that were analyzed. The graph shows that, although HVL values are rather small for low photon energies, they have begun to grow proportionally when photon energy is raised. Consequently, the HVL values for the S5 sample were the lowest of all the samples. For all glasses studied, the tenth value layer's (TVL) variability as a function of photon energy in MeV is shown in Figure 6. In all cases, the TVL parameter follows the same pattern as the HVL. Changes in the mean free path as a function of the incoming photon energy for glasses S1 through S5 are shown in Figure 7. This graph demonstrates that the concentration of Sb_2O_3 has a negative influence on the evolution of mean free path, which is an obvious indication of enhanced gamma-ray shielding characteristics. This is because of the decrease in the value of the mean free path implies that the distance between two successive gamma-ray contacts in the material reduces, indicating that the absorption process will be more efficient at shorter distances. Therefore, for a photon energy of 15 MeV, the values are lowest for the S5 glass sample and maximum for the S1 glass sample. Figures 8 and 9 demonstrate the gamma-ray energy (MeV)-dependent changes in the exposure build-up factor (EBF) and the energy absorption build-up factor (EABF) throughout a range of mean free path values, respectively. Both the EBF and EABF values are small in the low gamma-ray energy band because photoelectric absorption is responsible for the vast majority of entering gamma rays. Our results show that both EBF and EABF values decreased when Sb_2O_3 dosage was increased (i.e., from 0.5 to 40 mfp). The rate at which incident gamma rays collide with glass samples increases dramatically as the amount of Sb_2O_3 increases from S1 to S5. The gamma-ray TF values, which is a critical metric for shielding materials, was computed for S1, S2, S3, S4, and S5 glass samples for some well-known isotopes and their characteristic energies as ^{67}Ga (0.0086, 0.0093, 0.1840 MeV), ^{57}Co (0.0144, 0.1221, 0.1365 MeV), ^{111}In (0.0230, 0.1710, 0.2450 MeV), ^{133}Ba (0.0532, 0.0796, 0.0810, 0.2764, 0.3029, 0.3560, 0.3838 MeV), ^{201}Tl (0.0710, 0.1350, 0.1670 MeV), ^{99m}Tc (0.1405 MeV), ^{51}Cr (0.3201), ^{131}I (0.2843, 0.3645, 0.6370, 0.7229 MeV), ^{58}Co (0.5110, 0.8108 MeV), ^{137}Cs (0.6617 MeV), ^{60}Co (1.1732, 1.3325 MeV). The TF values of the glasses were calculated using two different methods. Initially, glass thicknesses were used to analyze the TF factors of samples S1 through S5. In addition, Figure 10 displays the radiation shielding parameters ACS and ECS. Figure 10 shows how the ECS varies as a function of the photon energy entering the system, whereas Figure 11 shows how the ACS varies. Figures 10 and 11 show that the ACS and ECS values decrease with increasing photon energy. In every glass tested, the ACS values are larger than the ECS values. This is because the likelihood of total atomic interaction in any material is greater than the probability of complete electrical contact with incoming photons. Figure 12 displays the transmission functions of the studied glasses as a function of radioisotope energy and glass thickness (MeV). As the radioisotope's energy rises, the TF shifts

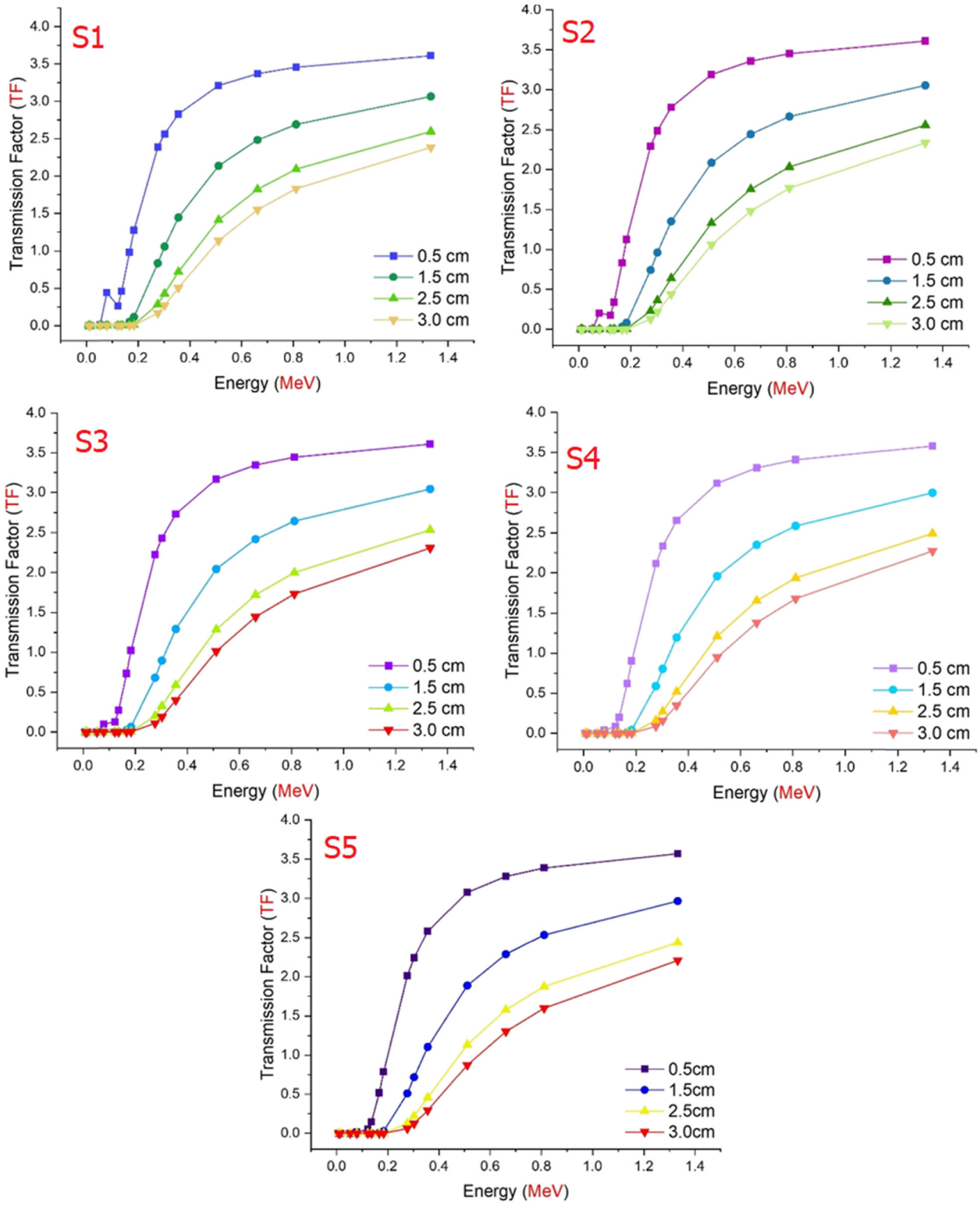

Figure 12: TFs of investigated glasses as a function of used radioisotope energy (MeV) at different glass thicknesses.

from 0.0086 to 1.3325 MeV. For all measured thicknesses, glass samples showed the lowest TF values when tested at low energies. Thicker samples may have an easier time attenuating low-energy gamma rays due to their high attenuation capacity. As a result, there is a significant difference of about 0.1 MeV. Glass samples become more

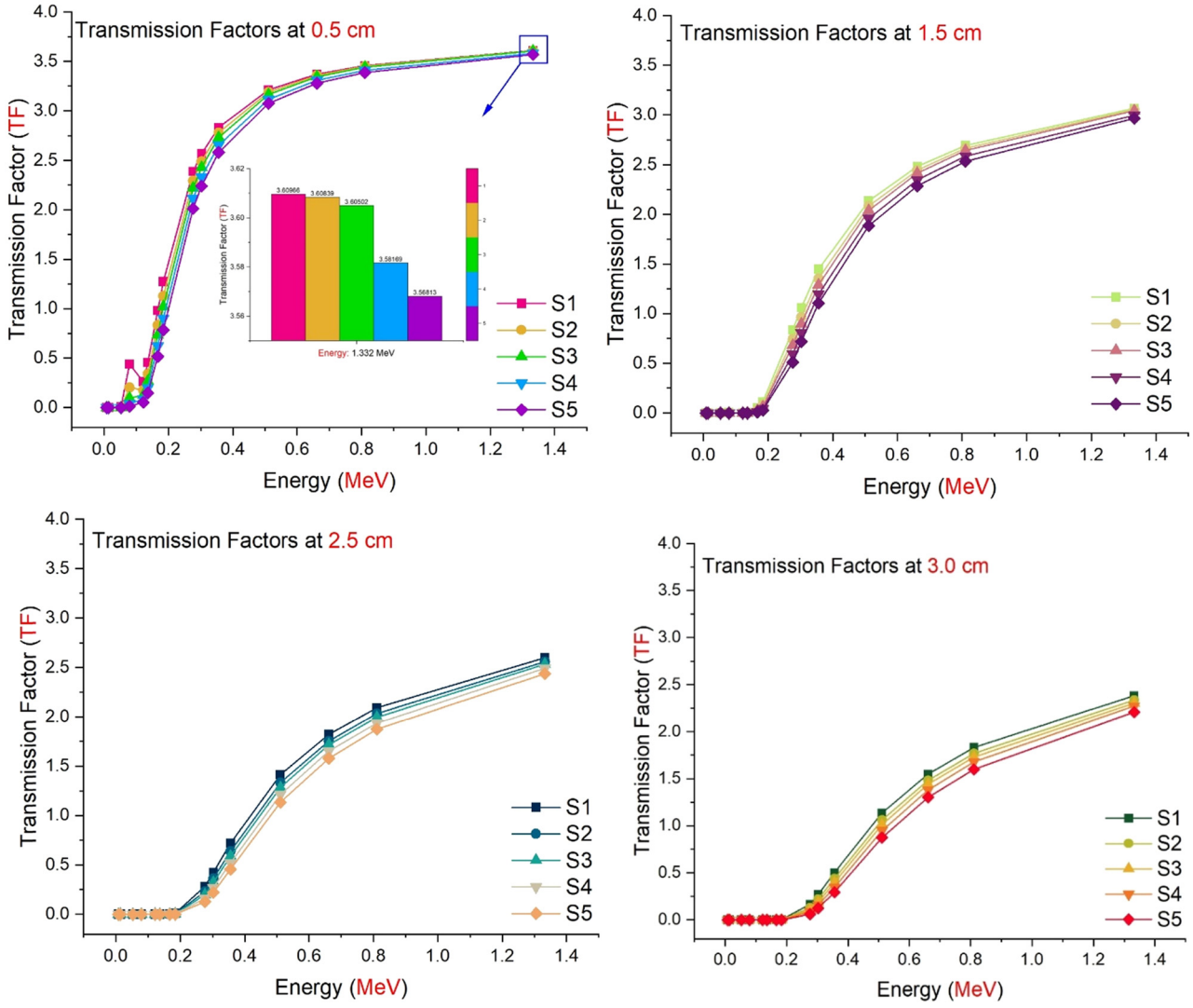

Figure 13: Comparison of the TFs as a function of used radioisotope energy (MeV) for different glass thicknesses.

reactive at gamma-ray energies greater than 0.1 MeV. Maximum attenuation was calculated for all glass samples at a thickness of 3 cm (i.e., minimum transmission). Increases in shield thickness have a negative effect on gamma-ray attenuation because shield thickness affects the effectiveness of any shielding material. The TF values of the glasses were then carefully assessed by considering the attenuation capabilities of various glass thicknesses (0.5, 1.5, 2.5, and 3 cm). Figure 13 displays the relationship between the transmitted energy (in MeV) and the glass thickness used for the experiment. The graph demonstrates the decline in TF values when gamma-ray energies are increased. The TF values of the glass samples examined were lowest for the thickness of 3 cm.

4 Conclusion

B_2O_3, which has the tendency to form glasses as combined with various compounds, is effectively being used in the making of new structures. Glass structures that B_2O_3 forms by uniting with heavy metal oxides make ground with their extraordinary properties in linear and nonlinear optics. In addition, combination of B_2O_3 with heavy metal PbO yields promising materials in radiation shielding. When Sb_2O_3 is used in industrial glasses at low ratios, it has the property to remove bubbles within the glass and decolorize special glasses. When they are found in the structure at high ratios, they have the property to rearrange the glass network; thus, it changes the

physical, optical, and structural properties of the glass to a high extent. The impact of gradual substitution of PbO with another heavy metal Sb_2O_3 in the glass network having Sb_2O_3–PbO–B_2O_3–CuO composition is found in the literature studies in which the examination of structural properties is prioritized. The effect of PbO/Sb_2O_3 change in the specified structure on radiation shielding properties was examined in this study in detail. Examining all radiation shielding parameters, we conclude that

1. The linear (μ) and mass attenuation (μ_m) coefficients trends as: $S5_{\mu,\mu m} > S4_{\mu,\mu m} > S3_{\mu,\mu m} > S2_{\mu,\mu m} > S1_{\mu,\mu m}$.
2. HVL, TVL, and MFP trends as: $S1_{HVL,TVLMFP} > S2_{HVL,TVL,MFP} > S3_{HVL,TVL,MFP} > S4_{HVL,TVL,MFP} > S5_{HVL,TVL,MFP}$.
3. Increasing the amount of Sb_2O_3 supplementation decreased the EBF and EABF levels in general (i.e., from 0.5 to 40 mfp). When the amount of Sb_2O_3 rises from S1 to S5, the collision rate of coming gamma rays in glass samples considerably increases.
4. The ACS and ECS values decrease when photon energy rises.
5. The ACS parameter values for all glasses are greater than the ECS parameter values. This is because the chance of full electronic contact with incoming photons is lower than the probability of complete atomic interaction in any substance.
6. According to the TF statistics, S5 exhibited the least transmission characteristic of all the investigated glass thicknesses.

Lastly, as a part of the scientific community's ongoing work on the current promising glass system, we would like to provide some ideas for future study that may be performed. After taking several factors into account, we were able to present detailed results in our investigation. A few significant material properties relate to glass materials; thus, although the proposed glassy system shows potential, it will require ongoing optimization and development. Based on the data obtained, a broad overview of the Sb_2O_3-containing glass samples was presented. However, due to the important material qualities connected with glass components, continued work is required in terms of overall optimization and development of the suggested glass system.

Funding information: The authors extend their appreciation to the Deputyship for Research & Innovation, Ministry of Education in Saudi Arabia, for funding this research work through the project number RI-44-0042.

Author contributions: Ghada ALMisned: writing, calculations, revision; Duygu Sen Baykal: calculations, writing, illustrations; Gokhan Kilic: calculations, writing; G. Susoy: calculations, writing, revision; Hesham M.H. Zakaly: calculations, writing; Antoaneta Ene: calculations, writing (the work of Antoaneta Ene and the APC were supported by Dunarea de Jos University of Galati, Romania through the grant no. RF 3621/2021); and Huseyin Ozan Tekin: writing, calculation, supervision, revision.

Conflict of interest: None.

Ethical approval: The conducted research is not related to either human or animal use.

Data availability statement: Data will be made available on request.

References

[1] Tekin HO, ALMisned G, Rammah YS, Susoy G, Ali FT, Sen Baykal D, et al. Mechanical properties, elastic moduli, transmission factors, and gamma-ray-shielding performances of Bi_2O_3–P_2O_5–B_2O_3–V_2O_5 quaternary glass system. Open Chem. 2022;20(1):314–29.

[2] Kim JH. Three principles for radiation safety: time, distance, and shielding. Korean J Pain. 2018;31(3):145–6. doi: 10.3344/kjp.2018.31.3.145.

[3] Tishkevich DI, Grabchikov SS, Grabchikova EA, Vasin DS, Lastovskiy SB, Yakushevich AS, et al. Modeling of paths andenergy losses of high-energy ions in single-layered and mul-tilayered materials. IOP Conf Ser Mater Sci Eng. 2020;848:012089. doi: 10.1088/1757-899X/848/1/012089.

[4] Saddeek YB. Ultrasonic and structural features of some borosilicate glasses. Bull Mater Sci. 2017;40(3):545–3.

[5] Radiation protection and safety of radiation sources: International basic safety standards. IAEA Gen Saf Requir. 2014;3:10–1.

[6] Lukoff J, Olmos J. Minimizing medical radiation exposure by incorporating a new radiation "Vital Sign" into the electronic medical record: Quality of care and patient safety. Perm J. 2017;21(4):17–007.

[7] Applying radiation safety standards in nuclear medicine. Safety reports series no. 40. Vienna: IAEA; 2005 (PDF) Diagnostic and therapeutic radioisotopes in nuclear medicine: Determination of gamma-ray transmission factors and safety competencies of high-dense and transparent glassy shields. Available from:https://www.researchgate.net/publication/361445714_Diagnostic_and_therapeutic_radioisotopes_in_nuclear_medicine_Determination_of_gamma-ray_transmission_factors_and_safety_competencies_of_high-dense_and_transparent_glassy_shields [accessed Sep 04 2022].

[8] Erdemir RU, Kilic G, Sen Baykal D, ALMisned G, Issa SA, Zakaly HM, et al. Diagnostic and therapeutic radioisotopes in nuclear medicine: Determination of gamma-ray transmission

factors and safety competencies of high-dense and transparent glassy shields. Open Chem. 2022;20(1):517–24.
[9] El-Batal HA, Ezz-El-Din FM. Interaction of γ-rays with Some alkali-alkaline-earth borate glasses containing chromium. J Am Ceram Soc. 1993;76(2):523–9.
[10] Abdel-Baki M, El-Diasty F. Role of oxygen on the optical properties of borate glass doped with ZnO. J Solid State Chem. 2011;184(10):2762–9.
[11] El-Falaky GE, Gaafar MS, Abd El-Aal NS. Ultrasonic relaxation in Zinc–Borate glasses. Curr Appl Phys. 2012;12(2):589–96.
[12] Sumalatha B, Omkaram I, Rajavardhana Rao T, Raju CL. Alkaline earth zinc borate glasses doped with Cu^{2+} ions studied by EPR, optical and IR techniques. J Non-Cryst Solids. 2011;357(16–17):3143–52.
[13] Kumar R, Rama AK, Bhatnagar J, Lakshmana R. EPR of vanadyl ions in alkali lead borate glasses. Mater Lett. 2002;57(1):178–82. doi: 10.1016/S0167-577X(02)00726-7.
[14] Rada M, Rada S, Pascuta P, Culea E. Structural properties of molybdenum-lead-borate glasses. Spectrochim Acta A Mol Biomol Spectrosc. 2010 Nov;77(4):832–7.
[15] Rao TR, Reddy CV, Krishna CR, Thampy UU, Raju RR, Rao PS, et al. Correlation between physical and structural properties of Co^{2+} doped mixed alkali zinc borate glasses. J Non-Cryst Solids. 2011;357(18):3373–80.
[16] Singh GP, Kaur P, Kaur S, Singh DP. Role of WO3 in structural and optical properties of WO_3–Al_2O_3–PbO–B_2O_3 glasses. Phys B. 2011;406(24):4652–6.
[17] Singh GP, Kaur S, Kaur P, Kumar S, Singh DP. Structural and optical properties of WO_3–ZnO–PbO–B_2O_3 glasses. Phys B. 2011;406(10):1890–3.
[18] Tekin HO, Issa SA, Kilic G, Zakaly HM, Badawi A, Bilal G, et al. Cadmium oxide reinforced $46V_2O_5$–$46P_2O_5$–$(8–x)B_2O_3$–xCdO semiconducting oxide glasses and resistance behaviors against ionizing gamma rays. J Mater Res Technol. 2021;13:2336–49.
[19] Tekin HO, Issa SA, Kilic G, Zakaly HM, Tarhan N, Sidek HA, et al. A systematical characterization of TeO_2–V_2O_5 glass system using boron (III) oxide and neodymium (III) oxide substitution: Resistance behaviors against ionizing radiation. Appl Sci (Basel). 2021;11(7):3035.
[20] Kilic G, Ilik E, Mahmoud KA, El-Mallawany R, El-Agawany FI, Rammah YS. Novel zinc vanadyl boro-phosphate glasses: ZnO–V_2O_5–P_2O_5–B_2O_3: Physical, thermal, and nuclear radiation shielding properties. Ceram Int. 2020;46(11, Part B):19318–27. doi: 10.1016/j.ceramint.2020.04.272.
[21] Kharita MH, Yousef S, AlNassar M. Review on the addition of boron compounds to radiation shielding concrete. Prog Nucl Energy. 2011;53(2):207–11. doi: 10.1016/j.pnucene.2010.09.012.
[22] Takaishi T, Jin J, Uchino T, Yoko T. Structural study of PbO–B_2O_3 glasses by X-ray diffraction and 11B MAS NMR techniques. J Am Ceram Soc. 2000;83(10):2543–8.
[23] Alothman MA, Kurtulus R, Olarinoye IO, Kavas T, Mutuwong C, Al-Buriahi MS. Optical, elastic, and radiation shielding properties of Bi_2O_3-PbO-B_2O_3 glass system: A role of SnO_2 addition. Opt (Stuttg). 2021;248:168047.
[24] Al-Buriahi MS, Kavaz E, Perişanoğlu U, Alalawi A, Çakıcı T, Alomairy S, et al. SrO effect on photon/particle radiation protection characteristics of SrO–PbO–B_2O_3 glasses. J Inorg Organomet Polym Mater. 2021;31(12):4546–62.
[25] Marzouk SY, Elbatal FH. Infrared and UV–visible spectroscopic studies of gamma-irradiated Sb_2O_3–B_2O_3 glasses. J Mol Struct. 2014;1063:328–5.
[26] ALMisned G, Tekin HO, Ene A, Issa SA, Kilic G, Zakaly HM. A closer look on nuclear radiation shielding properties of Eu^{3+} doped heavy metal oxide glasses: Impact of Al_2O_3/PbO substitution. Mater (Basel). 2021 Sep;14(18):5334.
[27] ALMisned G, Tekin HO, Issa SA, Ersundu MÇ, Ersundu AE, Kilic G, et al. Novel HMO-glasses with Sb_2O_3 and TeO_2 for nuclear radiation shielding purposes: A comparative analysis with traditional and novel shields. Mater (Basel). 2021 Aug;14(15):4330.
[28] Mostafa AM, Zakaly HM, Al-Ghamdi SA, Issa SA, Al-Zaibani M, Ramadan RM, et al. PbO–Sb_2O_3–B_2O_3–CuO glassy system: Evaluation of optical, gamma and neutron shielding properties. Mater Chem Phys. 2021;258:123937.
[29] Al-Hadeethi Y, Sayyed M. Effect of Gd_2O_3 on the radiation shielding characteristics of Sb_2O_3–PbO–B_2O_3–Gd_2O_3 glass system. Ceram Int. 2020;46(9):13768–73. doi: 10.1016/j.ceramint.2020.02.166.
[30] Doweidar H, El-Egili K, Ramadan R, Al-Zaibani M. Structural investigation and properties of Sb_2O_3–PbO–B_2O_3 glasses. J Non-Cryst Solids. 2018;497:93–101.
[31] Almatari M, Agar O, Altunsoy EE, Kilicoglu O, Sayyed MI, Tekin HO. Photon and neutron shielding characteristics of samarium doped lead alumino borate glasses containing barium, lithium and zinc oxides determined at medical diagnostic energies. Results Phys. 2019;12:2123–8.
[32] Tekin HO, ALMisned G, Susoy G, Ali FT, Baykal DS, Ene A, et al. Transmission Factor (TF) behavior of Bi_2O_3–TeO_2–Na_2O–TiO_2–ZnO glass system: A Monte Carlo simulation study. Sustainability (Basel). 2022;14(5):2893.
[33] Computer Code Collection RS. MCNPX user's manual version 2.4.0. Monte Carlo N-particle transport code system for mul-tiple and high energy applications, 2002.
[34] Tekin HO, Issa SAM, Kavaz E, Guclu EEA. The direct effect of Er_2O_3 on bismuth barium telluro borate glasses for nuclear security applications. Mater Res Express. 2019;6(11):115212.
[35] Mahmoud IS, Issa SAM, Saddek YB, Tekin HO, Kilicoglu O, Alharbi T, et al. Gamma, neutron shielding and mechanical parameters for vanadium lead vanadate glasses. Ceram Int. 2019;45:14058–72.
[36] Tekin HO, Kassab LR, Kilicoglu O, Magalhães ES, Issa SA, da Silva Mattos GR. Newly developed tellurium oxide glasses for nuclear shielding applications: an extended investigation. J Non-Cryst Solids. 2020;528:119763.
[37] Sayyed MI, Kumar A, Tekin HO, Kaur R, Singh M, Agar O, et al. Evaluation of gamma-ray and neutron shielding features of heavy metals doped Bi_2O_3-BaO-Na_2O-MgO-B_2O_3 glass systems. Prog Nucl Energy. 2020;118:103118.
[38] Rammah YS, Ashok Kumar KA, Mahmoud R, El-Mallawany F, El-Agawany I, Susoy G, et al. SnO reinforced silicate glasses and utilization in gamma radiation shielding applications. Emerg Mater Res. 2020;9(3):1000–8. doi: 10.1680/jemmr.20.00150.
[39] Agar O, Kavaz E, Altunsoy EE, Kilicoglu O, Tekin HO, Sayyed MI, et al. Nevzat Tarhan. Er_2O_3 effects on photon and neutron shielding properties of TeO_2-Li_2O–ZnO-Nb_2O_5 glass system. Results Phys. 2019;13:102277.

[40] Rashad M, Tekin HO, Zakaly HMH, Pyshkina M, Issa SAM, Susoy G. Physical and nuclear shielding properties of newly synthesized magnesium oxide and zinc oxide nanoparticles. Nucl Eng Technol. 2020;52(9):2078–84.
[41] Sharma A, Sayyed MI, Agar O, Tekin HO. Simulation of shielding parameters for TeO_2-WO_3-GeO_2 glasses using FLUKA code. Results Phys. 2019;13:102199.
[42] Rammah Y, Issa SAM, Zakaly H, Tekin HO, Yousef E, Abouhaswa AS. B_2O_3-Bi_2O_3-Li_2O_3-Cr_2O_3 glasses: fabrication, structure, mechanical, and gamma radiation shielding qualities. J Aust Ceram Soc. 2021;57(4):1057–69. doi: 10.1007/s41779-021-00599-w.
[43] Issa SAM, Tekin HO, Hessien MM, Rammah YS. Investigation of the elastic moduli, optical characteristics, and ionizing radiation attenuation capacity of specific strontium borosilicate glasses. J Aust Ceram Soc. 2022;58(2):495–510. doi: 10.1007/s41779-022-00706-5.
[44] Tekin HO, Rammah YS, Hessien MM, Zakaly HMH, Issa SAM. Evaluating the optical and gamma-ray protection properties of bismo-tellurite sodium titanium zinc glasses. J Aust Ceram Soc. 2022 Mar;26(3):851–66.
[45] ALMisned G, Akkurt I, Tekin HO, Erdamar IYD, Dogan SO. Gamma ray shielding properties of CeO_2-added hydroxyapatite composite. J Aust Ceram Soc. 2022;58(4):1209–17. doi: 10.1007/s41779-022-00763-w.